Analytical Methods

PAPER

View Article Online
View Journal | View Issue

CrossMark click for updates

Cite this: *Anal. Methods*, 2015, **7**, 8004

A guanidinium modified rhodamine-based fluorescent probe for *in vitro*/*vivo* imaging of gold ions†

Erman Karakuş,[a] Gulcin Cakan-Akdogan[b] and Mustafa Emrullahoğlu*[a]

Received 19th June 2015
Accepted 1st August 2015

DOI: 10.1039/c5ay01581b

www.rsc.org/methods

We devised a rhodamine-based fluorescent probe functionalized with a guanidinium moiety, which both operates efficiently in pure aqueous media and displays a selective fluorescence response to Au^{3+} ions. We also demonstrated the successful fluorescence imaging of Au^{3+} within living cells and a vertebrate species, the zebrafish.

Published on 18 August 2015. Downloaded by Izmir Yuksek Teknoloji on 18/07/2017 13:58:47.

Introduction

Ionic gold species facilitate remarkable chemical and biological activities. Recently, using gold as a catalyst has attracted great interest in the field of synthetic chemistry.[1–5] Yet, along with their synthetic utility, gold species exert diverse biological effects on human health, ranging from disease treatment to organ damage.[6–10] Drugs based on certain gold-ion complexes can be used to treat various human diseases, including asthma, cancer, and rheumatoid arthritis, among other autoimmune diseases. However, in sharp contrast to their beneficial effects, gold ions also have the potential to disturb a range of biological processes as they bind strongly to biomolecules, thereby causing serious health problems and damage to organs.[9,10]

The design and development of molecular tools for detecting biologically important target species is an alluring subject of research in the area of chemosensing and molecular imaging.[11–17] Apart from the biological significance of gold ions, the focus of recent research has been on the development of probes that can simply identify gold species in the living milieu.

Lately, we and also other researchers have devised a series of molecular sensors that proved highly efficient in monitoring gold ions in chemical and biological environments. Given their impressive photophysical properties, fluorescent molecules such as rhodamine,[17–23] boron-dipyrromethene (BODIPY),[24–27] fluorescein[28–30] and naphthalimide[31,32] are most commonly employed as signal transducers.

Notably, the great majority of those probes use an alkyne motif as a gold ion-recognition site and benefit from the strong alkyne affinity of gold ions to modulate an optical signal. Alternative sensing events such as C=N bond hydrolysis[25–27] and reversible ion–dipole interactions[21] have also been employed for signal modulation. However, several challenges continue to impede the optimum performance of such sensing systems, for example, chronical interference of other metal ions. In addition, since most sensors are not completely soluble in pure water, they require a mixture of solvent systems that can, in turn, dramatically limit their usefulness for biological purposes. Another problem is the prolonged incubation time required to measure any reliable signal change, because only a few can discriminate gold ions of different oxidation states,[21,26,31] which is nevertheless crucial for studying the redox states of the ions. As such, to overcome general barriers in gold ion sensing, it is essential to propose new types of fluorescent molecules that use alternative recognition strategies and moieties for detecting gold ions.

Among the known fluorescent molecules, the rhodamine framework, given its unique signal modulation property, is an excellent candidate for constructing off–on type fluorescent sensors. Depending on the conditions, the spirocyclic rhodamine derivative can exist in two isomeric forms. In the closed isomeric form, the dye is non-fluorescent and colourless, whereas in the open amide form, the dye gains a characteristic pink colour and displays a strong fluorescence emission. This unique behaviour of rhodamine has been exploited as a signal modulation mechanism in chemosensor design.[33–36]

Here, we present a novel gold ion selective fluorescent probe based on a spirocyclic rhodamine dye with favourable properties, including a fast response (<30 s) at room temperature, operability in pure water, cell membrane permeability, and the ability to differentiate Au^{3+} from Au^{+}.

Our sensor design involves constructing a spirocyclic rhodamine dye modified with a guanidine motif as a gold ion-recognition site. Based on the studies that used guanidine derivatives as coordinating ligands for gold ions,[37,38] we envisioned that a guanidine motif on the rhodamine dye would aid the specific recognition of gold ions (Fig. 1). Moreover, we

[a]*Department of Chemistry, Faculty of Science, İzmir Institute of Technology, Urla, 35430, İzmir, Turkey. E-mail: mustafaemrullahoglu@iyte.edu.tr*

[b]*Dokuz Eylül University, İzmir Biomedicine and Genome Center, İzmir, Turkey*

† Electronic supplementary information (ESI) available: Synthesis and characterization of **Rh-EDC**, and all data for UV-Vis and fluorescence titrations. See DOI: 10.1039/c5ay01581b

This journal is © The Royal Society of Chemistry 2015

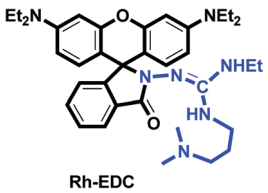

Fig. 1 Molecular structure of Rh-EDC.

Published on 18 August 2015. Downloaded by Izmir Yuksek Teknoloji on 18/07/2017 13:58:47.

speculated that the guanidine motif, capable of forming strong hydrogen bonds with water, would also improve the solubility of the probe in water and eliminate the need for a cosolvent.

Experimental

Synthesis of Rh-EDC

To a solution of rhodamine B hydrazide (100 mg, 0.22 mmol) in absolute ethanol (5 mL) 1-ethyl-3-(3-dimethylamino-propyl) carbodiimide (68 mg, 0.44 mmol) was added. The solution was stirred overnight at reflux temperature. The reaction mixture was extracted with dichloromethane (3 × 10 mL). Then the collected organic layers were dried over anhydrous $MgSO_4$, concentrated under vacuum, and purified by column chromatography (dichloromethane/methanol = 10/1) to give 28 mg of **Rh-EDC** (20%) as a pink solid. ^{1}H-NMR (400 MHz, $CDCl_3$) δ: 9.20 (br. s, 1H), 7.96 (s, 1H), 7.68–7.60 (m, 2H), 7.29 (d, J = 7.6 Hz, 1H), 6.40–6.37 (m, 4H), 6.30–6.28 (m, 2H), 4.66 (br. s, 1H), 3.39–3.20 (m, 14H), 2.37 (br. s, 2H), 1.88 (br. s, 6H), 1.15 (t, J = 6.8 Hz, 12H), 0.87 (t, J = 6.0 Hz, 3H). ^{13}C NMR (100 MHz, $CDCl_3$) δ: 165.6, 157.3, 154.7, 149.2, 148.9, 133.9, 130.1, 129.1, 127.7, 124.7, 123.6, 107.8, 104.9, 97.9, 67.2, 52.9, 44.4, 42.5, 38.6, 37.6, 29.9, 26.0, 14.0, 12.5. HRMS: m/z: calcd for $C_{36}H_{49}N_7O_2$: 612.40271 $[M + H]^+$, found: $[M + H]^+$ 612.40205.

Cell imaging

Human A549 lung adenocarcinoma cell lines were grown in DMEM (Dulbecco's modified eagle medium) supplemented with 10% FBS (fetal bovine serum) in an atmosphere of 5% CO_2 at 37 °C. The cells were plated on 12 mm cover glasses in a 6-well plate and allowed to grow for 24 h. Before the experiments, the cells were washed with PBS (0.1 M) buffer, then the cells were incubated with **Rh-EDC** (10 μM) for 20 min at 37 °C and then washed with PBS three times. After incubating with Au^{3+} (10 μM) for 20 min at 37 °C, the cells were rinsed with PBS three times, and with DAPI (4′,6-diamidino-2-phenylindole) for 15 min at 37 °C, and then washed with PBS three times. Then the fluorescence images were acquired by using a fluorescence microscope.

Zebrafish imaging

Zebrafish embryos were maintained in E2 embryo medium (15 mM NaCl, 0.5 mM KCl, 1 mM $MgSO_4$, 1 mM $CaCl_2$, 0.15 mM KH_2PO_4, 0.05 mM Na_2HPO4, 0.7 mM $NaHCO_3$, pH 7.5) including 0.5% methylene blue. Embryos were dechorionated manually at 2 dpf (days post fertilization), and incubated with 10 μM **Rh-EDC** in E2 medium for 20 min at 28 °C. After washing with E2 for 4 × 5 min to remove the remaining **Rh-EDC**, the embryos were further treated with 20 μM of Au^{3+} in E2 media for 20 min at 28 °C. Unbound Au^{3+} was washed for 4 × 5 min with E2. The embryos were mounted in 3% methylcellulose with tricaine and imaged by using an Olympus SZX16 stereomicroscope.

Results and discussion

Synthetic scheme

The title compound, **Rh-EDC**, was prepared synthetically as outlined in Scheme 1. Rhodamine hydrazide (**1**) was prepared by reacting rhodamine B with hydrazine hydrate in ethanol at reflux temperature. Rhodamine hydrazide was then treated with EDC [1-ethyl-3-(3-dimethylaminopropyl) carbodiimide] in ethanol under reflux conditions, which produced the title compound (isolated yield 20%). After chromatographic purification, the structure of the probe was clearly confirmed by nuclear magnetic resonance (NMR) and high-resolution mass spectrometry (HRMS) analysis.[39]

Au^{3+} sensing properties of Rh-EDC

We commenced our investigation by analysing the most efficient environment for the sensing event. In general, spirolactam derivatives of rhodamine, bearing aromatic or aliphatic amide units in their molecular structure, hardly dissolve in water. Typically, a considerable amount of an organic cosolvent is thus required to improve the solubility. Notably, **Rh-EDC**, here modified with a guanidine motif, was completely soluble in water, thereby eliminating the need for a cosolvent.

A prominent limitation of rhodamine-based chemosensors is the sensitivity of the rhodamine spirolactam ring to acidity changes. Mostly, the spirolactam-ring of rhodamine is prone to transformation into its open isomeric form upon protonation, which can interfere with the detection of the analyte species. To rule out any discrepancies arising from acidity changes, we investigated the effect of pH fluctuations on the fluorescence behaviour of the sensing system, and found that **Rh-EDC** was insensitive to pH fluctuations (pH 2.0–12.0). The detection of gold ions by **Rh-EDC** was also not disturbed by changing the pH of the sensing media, indicating that **Rh-EDC** could properly detect Au^{3+} across a wide pH range (Fig. S8, ESI†). Based on these findings, a reaction medium buffered to pH 7.0 was chosen for physiological applications.

With the aid of UV and fluorescence spectroscopy, we systematically studied the probe's spectroscopic behaviour upon reaction with added metal species. Free **Rh-EDC** was colourless in solution, exhibited no visible absorption peak, and

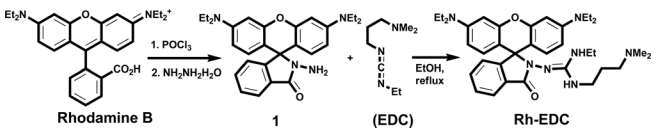

Scheme 1 Synthesis of Rh-EDC.

Published on 18 August 2015. Downloaded by Izmir Yuksek Teknoloji on 18/07/2017 13:58:47.

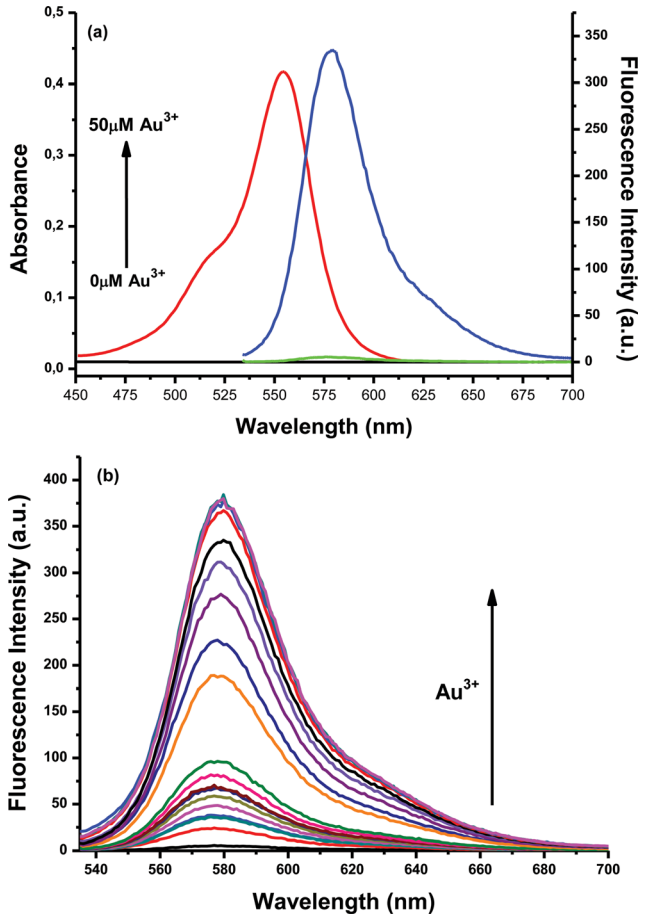

Fig. 2 (a) Absorbance spectra of **Rh-EDC** (10 μM) in the absence (black line) and presence (red line) of 5 equiv. of Au^{3+} and fluorescence spectra of **Rh-EDC** (10 μM) in the absence (green line) and presence (blue line) of 5 equiv. of Au^{3+} in phosphate buffer (0.1 M) at pH 7.0. (b) Emission titration curve of **Rh-EDC** (10 μM) and Au^{3+} (0 to 10 equiv.) in phosphate buffer (0.1 M) at pH 7.0 (after 5 min).

was non-fluorescent, indicating that the spirolactam ring was preserved. Upon adding Au^{3+} to the **Rh-EDC** solution, a new absorption peak emerged at 554 nm, and the colour of the probe solution became brilliant pink. Meanwhile, a new emission band became centred at 580 nm in the fluorescence spectrum, suggesting that the spirolactam ring of the probe structure was transformed into its open form (Fig. 2(a)).

The intensity of fluorescence emission at 580 nm increased linearly with an increasing concentration of Au^{3+} across a wide concentration range (Fig. S4 and S5, ESI†). **Rh-EDC** responded to the addition of Au^{3+} in 30 s ($k_{obs} = 1.37 \times 10^{-2}$ s^{-1}), and the enhancement of the emission intensity (>75 fold) became saturated within a couple of minutes when 1 equiv. of Au^{3+} was added (Fig. S2 and S3, ESI†). At the same time, the detection limit of **Rh-EDC** for detecting Au^{3+} was 2.0 nM, based on the signal-to-noise ratio (S/N = 3) (Fig. S9, ESI†).

Selectivity studies

The sensitivity of **Rh-EDC** to other possible metal species, including Au^{+}, Pd^{2+}, Hg^{2+}, Cu^{2+}, Zn^{2+}, Ba^{2+}, Pb^{2+}, Ni^{2+}, Na^{+}, Mg^{2+}, Li^{+}, K^{+}, Ag^{+}, Cd^{2+}, Ca^{2+}, Fe^{3+}, and Cr^{3+} was investigated under the same sensing conditions. For all other metal species tested, no obvious spectral changes were observed. Fortunately, Ag^{+}, Hg^{2+}, and Pd^{2+}, the three most competitive metal species for detecting gold species, did not cause any spectral change. Furthermore, no change was detected in the spectrum when Au^{+} ions were present, showing that **Rh-EDC** allows the successful discrimination of Au^{3+} from Au^{+} (Fig. 3).

Au^{3+} species are prone to react with thiol species to form thiol complexes of gold ions. This kind of transformation could make it highly challenging to realize gold species in a biological system. It was thus highly essential to investigate the spectral response of the probe toward Au^{3+} in the presence of reactive biothiol species, such as cysteine, the most nucleophilic and chemically reactive among the common amino acids. Meanwhile, we have also examined the interference of other metal ions with the selectivity of **Rh-EDC**. The results from the competition experiments showed that **Rh-EDC** could smoothly detect Au^{3+} ions in the mixtures of other related species (Fig. S7, ESI†).

To clarify the nature of the sensing process, we first questioned whether it is reversible. To this end, CN^{-} ions were introduced into the solution of **Rh-EDC** pre-treated with Au^{3+}.

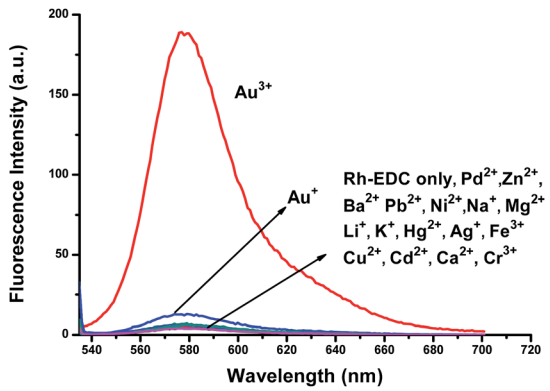

Fig. 3 Fluorescence intensities of **Rh-EDC** (10 μM) in phosphate buffer (0.1 M) at pH = 7.0, emission at 580 nm (λ_{ex}: 515 nm): in the presence of Au^{3+} (1 equiv.) and other metal ions (10 equiv.) after 5 min.

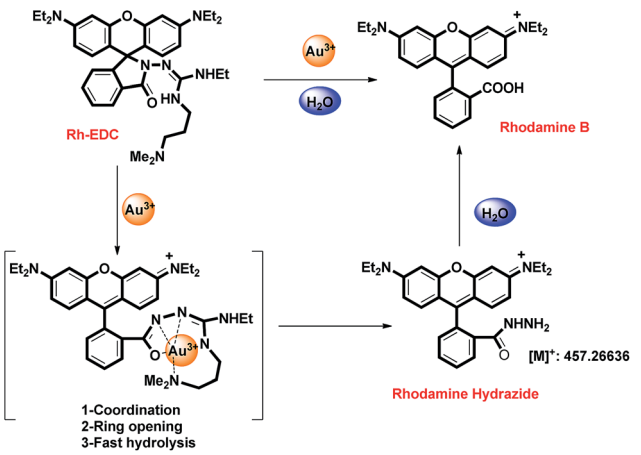

Scheme 2 Proposed mechanism for the detection of Au^{3+} ions.

This journal is © The Royal Society of Chemistry 2015

Published on 18 August 2015. Downloaded by Izmir Yuksek Teknoloji on 18/07/2017 13:58:47.

Interestingly, even after the addition of an excessive amount of cyanide ions, the solution preserved its colour and emission, suggesting that the sensing process might be based on an irreversible chemical reaction mediated by gold ions.

Reaction mechanism

The outcome of the sensing process could be easily observed by thin-layer chromatography (TLC). The appearance of an orange emissive compound on the TLC plate strongly suggested the formation of a new rhodamine derivative (Fig. S10, ESI†). With the aid of NMR spectroscopy, the structure of this new compound was confirmed to be rhodamine B, the hydrolysis product of **Rh-EDC**.[39] HRMS analysis of the probe solution (probe + Au^{3+}) elucidated the sensing mechanism by showing two molecular ion peaks at *m*/*z* 443.23 and 457.26, attributed respectively to rhodamine-B and rhodamine hydrazide.

As illustrated in Scheme 2, the sensing mechanism is thought to proceed from the simultaneous coordination of Au^{3+} with the ligand and dye, which promotes the opening of the spiro-amide ring. Specifically, rapid hydrolysis of the C=N bond *via* the attack of water results first in the formation of rhodamine hydrazide, which further hydrolyses to rhodamine B, thereby producing the distinct colour and emission of the solution.

Cell and zebrafish imaging

Since **Rh-EDC** displayed nearly all desirable features necessary for recognizing gold ions in the living milieu, we assessed the capacity of **RH-EDC** to track gold species in living cells. To this end, lung adenocarcinoma cells (A-549) were first incubated with **Rh-EDC** (10 μM), to which was added Au^{3+} (10 μM) and incubated for another 20 min. The cells were stained with a nucleus staining dye (DAPI) for another 15 min, and fluorescence images were taken with and without Au^{3+} (10 μM). As Fig. 4 shows, the human lung adenocarcinoma (A549) cells incubated with **Rh-EDC** did not display any fluorescence in the absence of Au^{3+} species. Based on the nucleus counter stain and the red fluorescence emitting from the cells, we thus conclude that the probe passes through the cell membrane and detects Au^{3+} from within the cell, particularly in the cytosol.

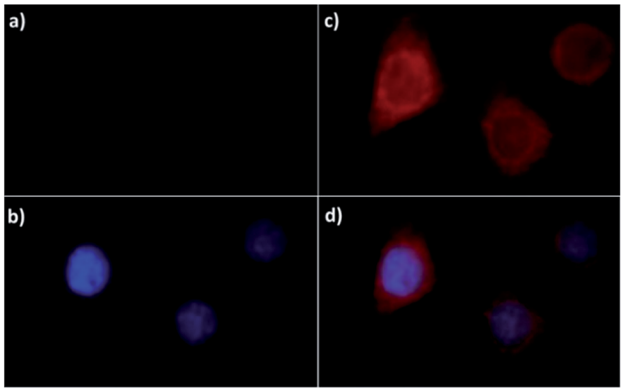

Fig. 4 Images of A-549 cells: cells treated with **Rh-EDC** (10 μM) in the absence of Au^{3+} (control) do not have any fluorescent signal (a), although cells are detected with the DAPI nuclear counter-stain as shown in the merged image (b). Cells treated with **Rh-EDC** (10 μM) and Au^{3+} (10 μM) display strong red fluorescence (c), the fluorescence signal appears in and around of the nucleus judged by the DAPI counter stain in the merged image (d). DAPI blue, **Rh-EDC** red.

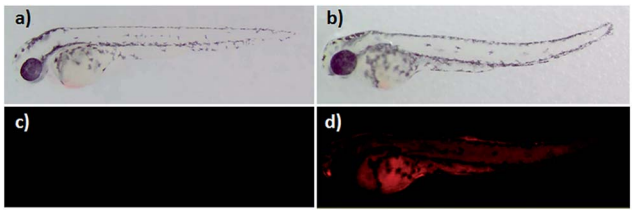

Fig. 5 Bright field microscopic images of zebrafish embryos treated with (a) **Rh-EDC** (10 μM) in the absence of Au^{3+}, and (b) **Rh-EDC** (10 μM) and Au^{3+} (20 μM). Fluorescence images of zebrafish embryos treated with (c) **Rh-EDC** (10 μM) (control) and (d) **Rh-EDC** (10 μM) and Au^{3+} (20 μM) showing that **Rh-EDC** fluoresces in the embryo only in the presence of Au^{3+}.

Encouraged by the success of the cell imaging studies, we next questioned the potential of the probe to detect Au^{3+} ions in living organisms. Though *in vivo* fluorescence sensing of certain metal species such as Hg^{2+}, Cu^{2+}, Pd^{2+}, and Zn^{2+} has previously been reported, tracking gold ions in a living organism, particularly in zebrafish, with fluorescent probes has not been investigated before. In fact, to the best of our knowledge, this is the first report to describe a fluorescence-based method for monitoring gold ions *in vivo*.

The species of zebrafish was chosen as a vertebrate animal model chiefly due to its small size and optical transparency. For the imaging studies, zebrafish embryos 2dpf (days post fertilization) were pre-incubated with **Rh-EDC** (10 μM) for 20 min, unbound **Rh-EDC** was washed out and embryos were incubated with 20 μM Au^{3+} for another 20 min. As Fig. 5 shows, no signs of fluorescence emission emerged in the specimen in the absence of external gold ions. However, upon adding gold ions, strong fluorescence intensity was observed throughout the body and yolk of the embryo, indicating that the probe and Au^{3+} species interacted within the organism to form a highly fluorescent product, consistent with the results obtained in the solution. This preliminary study with living organisms and their cells established that the probe can smoothly enter living cells and zebrafish and, once inside, it can track gold species in the living milieu.

Conclusions

In sum, we have developed a rhodamine-based, off-on type fluorescent probe showing a remarkable fluorescence change in response to Au^{3+} ions with high sensitivity and selectivity over other metal ions. Remarkably, this probe is soluble in pure water, insensitive to pH fluctuations, and efficiently operable under physiological conditions, which is of crucial importance for biological imaging studies. Moreover, it displays high specificity for Au^{3+} ions with an extremely low detection limit—by far the lowest detection limit reported in gold ion sensing.

Published on 18 August 2015. Downloaded by Izmir Yuksek Teknoloji on 18/07/2017 13:58:47.

Apart from the rapid and specific response to Au^{3+} in the solution, this probe proved highly successful in imaging gold species in both living cells and living organisms.

Acknowledgements

The authors gratefully acknowledge IZTECH (İzmir Institute of Technology) and TUBITAK (113Z601) for financial support.

Notes and references

1 I. Braun, A. M. Asiri and A. S. K. Hashmi, *ACS Catal.*, 2013, **3**, 1902.
2 Z. Li, C. Brouwer and C. He, *Chem. Rev.*, 2008, **108**, 3239.
3 A. Arcadi, *Chem. Rev.*, 2008, **108**, 3266.
4 A. S. K. Hashmi and M. Rudolph, *Chem. Soc. Rev.*, 2008, **37**, 1766.
5 N. Krause and C. Winter, *Chem. Rev.*, 2011, **111**, 1994.
6 C. F. Shaw III, *Chem. Rev.*, 1999, **99**, 2589.
7 I. Ott, *Coord. Chem. Rev.*, 2009, **253**, 1670.
8 M. Navarro, *Coord. Chem. Rev.*, 2009, **253**, 1619.
9 C. M. Goodman, C. D. McCusker, T. Yilmaz and V. M. Rotello, *Bioconjugate Chem.*, 2004, **15**, 897.
10 A. Habib and M. Tabata, *J. Inorg. Biochem.*, 2004, **98**, 1696.
11 S. Singha, D. Kim, H. Seo, S. W. Cho and K. H. Ahn, *Chem. Soc. Rev.*, 2015, **44**, 4367.
12 K. P. Carter, A. M. Young and A. E. Palmer, *Chem. Rev.*, 2014, **114**, 4564.
13 X. Li, X. Gao, W. Shi and H. Ma, *Chem. Rev.*, 2014, **114**, 590.
14 Z. Guo, S. Park, J. Yoon and I. Shin, *Chem. Soc. Rev.*, 2014, **43**, 16.
15 Y. Yang, Q. Zhao, W. Feng and F. Li, *Chem. Rev.*, 2013, **113**, 192.
16 O. A. Bozdemir, R. Guliyev, O. Buyukcakir, S. Selcuk, S. Koleman, G. Gulseren, T. Nalbantoglu and E. U. Akkaya, *J. Am. Chem. Soc.*, 2010, **132**, 8029.
17 M. J. Jou, X. Chen, K. M. K. Swamy, H. N. Kim, H.-J. Kim, S. G. Lee and J. Yoon, *Chem. Commun.*, 2009, 7218.
18 O. A. Egorova, H. Seo, A. Chatterjee and K. H. Ahn, *Org. Lett.*, 2010, **12**, 401.
19 Y. K. Yang, S. Lee and J. Tae, *Org. Lett.*, 2009, **11**, 5610.
20 L. Yuan, W. Lin, Y. Yang and J. Song, *Chem. Commun.*, 2011, **47**, 4703.
21 J. Wang, W. Lin, L. Yuan, J. Song and W. Gao, *Chem. Commun.*, 2011, **47**, 12506.
22 M. Emrullahoğlu, E. Karakuş and M. Üçüncü, *Analyst*, 2013, **138**, 3638.
23 H. Seo, M. E. Jun, K. Ranganathan, K.-H. Lee, K.-T. Kim, W. Lim, Y. M. Rhee and K. H. Ahn, *Org. Lett.*, 2014, **16**, 1374.
24 J.-B. Wang, Q.-Q. Wu, Y.-Z. Min, Y.-Z. Liu and Q.-H. Song, *Chem. Commun.*, 2012, **48**, 744.
25 E. Karakuş, M. Üçüncü and M. Emrullahoğlu, *Chem. Commun.*, 2014, **50**, 1119.
26 M. Üçüncü and M. Emrullahoğlu, *Chem. Commun.*, 2014, **50**, 5884.
27 C. Cantürk, M. Üçüncü and M. Emrullahoğlu, *RSC Adv.*, 2015, **5**, 30522.
28 H. Seo, M. E. Jun, O. A. Egorova, K. H. Lee, K. T. Kim and K. H. Ahn, *Org. Lett.*, 2012, **14**, 5062.
29 N. Y. Patil, V. S. Shinde, M. S. Thakare, P. H. Kumar, P. R. Bangal, A. K. Barui and C. R. Patra, *Chem. Commun.*, 2012, **48**, 11229.
30 S. Kambam, B. Wang, F. Wang, Y. Wang, H. Chen, J. Yin and X. Chen, *Sens. Actuators, B*, 2015, **209**, 1005.
31 M. Dong, Y.-W. Wang and Y. Peng, *Org. Lett.*, 2010, **12**, 5310.
32 J. Y. Choi, G.-H. Kim, Z. Guo, H. Y. Lee, K. M. K. Swamy, J. Pai, S. Shin, I. Shin and J. Yoon, *Biosens. Bioelectron.*, 2013, **49**, 438.
33 H. N. Kim, M. H. Lee, H. J. Kim, J. S. Kim and J. Yoon, *Chem. Soc. Rev.*, 2008, **37**, 1465.
34 M. Beija, C. A. M. Afonso and J. G. Martinho, *Chem. Soc. Rev.*, 2009, **38**, 2410.
35 X. Chen, T. Pradhan, F. Wang, J. S. Kim and J. Yoon, *Chem. Rev.*, 2012, **112**, 1910.
36 H. Zheng, X.-Q. Zhan, Q.-N. Bian and X.-J. Zhang, *Chem. Commun.*, 2013, **49**, 429.
37 H. J. Zawadzki, *Transition Met. Chem.*, 2003, **28**, 820.
38 D. Emeljanenko, A. Peters, V. Vitske, E. Kaifer and H.-J. Himmel, *Eur. J. Inorg. Chem.*, 2010, 4783.
39 See ESI for more details.†

 This journal is © The Royal Society of Chemistry 2015